J Neuropathol Exp Neurol

Vol. 70, No. 8
August 2011
pp. 678–685

ORIGINAL ARTICLE

Peripheral Neuropathy Is Linked to a Severe Form of Myotonic Dystrophy in Transgenic Mice

Petrica-Adrian Panaite, MD, PhD, Marie Kielar, MS, Rudolf Kraftsik, MS, Geneviève Gourdon, PhD, Thierry Kuntzer, MD, and Ibtissam Barakat-Walter, PhD

Abstract

Myotonic dystrophy type 1 (DM1) is a multisystem disorder with a variable phenotype. The involvement of peripheral nerves in DM1 disease is controversial. The DM1 animal model DM300 transgenic mice that carry 350 to 500 CTG repeats express a mild DM1 phenotype but do not exhibit motor or sensory pathology. Here, we investigated the presence or absence of peripheral neuropathy in transgenic mice (DMSXL) that carry more than 1,300 CTG repeats and display a severe form of DM1. Electrophysiologic, histologic, and morphometric methods were used to investigate the structure and function of peripheral nerves. We observed lower compound muscle action potentials recorded from hind limb muscles and slowing of sciatic nerve conduction velocity in DMSXL versus control mice. Morphometric analyses showed an axonopathy and neuronopathy in the DMSXL mice characterized by a decrease in numbers of myelinated motor axons in sciatic nerve and in spinal cord motor neurons. Pathologic alterations in the structure of hind limb neuromuscular junctions were also detected in the DMSXL mice. These results suggest that peripheral neuropathy can be linked to a large CTG expansion and a severe form of DM1.

Key Words: Compound muscle action potential, DMSXL transgenic mice, Motor neuropathy, Myotonic dystrophy, Neuromuscular junctions, Physical disector method.

INTRODUCTION

Myotonic dystrophy type 1 (DM1) is a multisystemic autosomal dominant disorder with a highly variable clinical phenotype (1, 2). The genetic basis for DM1 is the abnormal amplification of a cytosine-thymine-guanine (CTG) trinucleotide repeat in the 3′ untranslated region of the DM protein kinase (*DMPK*) gene on chromosome 19q (3, 4). The number of DNA CTG repeats usually increases in successive generations of DM1 families, and the size of triplet correlates with the severity of the disease. In healthy individuals without DM1, 5 to 35 copies of repeat have been observed. Patients with CTG expansion containing 50 to 80 CTG repeats are almost asymptomatic. Individuals with 100 to 1,000 CTG repeats develop a disease in adult life (the classic form of DM1) that is characterized by progressive muscle wasting with myotonia. However, the most severe form of DM1 is congenital disease; the mutation becomes unstable, and after 3 to 4 generations, the CTG repeat lengthens to up to 2,000 repeats (5). This form of disease is characterized by extreme myotonia and muscular atrophy (6). Other systemic manifestations such as cataracts, cardiac conduction defects, endocrine dysfunction, respiratory failure, and changes in the CNS with mental retardation and hypersomnia are recognized as common extramuscular manifestations in patients with DM1 (2, 7–11). Although a number of clinical reports have drawn attention to the occasional presence of a peripheral neuropathy in patients with DM1 (12–16), other reports dispute completely the presence of neuropathy in patients (17–21). Therefore, additional studies are needed to determine the involvement of the peripheral nervous system (PNS) in DM1.

During the last few years, the use of animal models for studying DM1 mechanisms has become more frequent because access to the nervous system is only possible at the end stage of the disease. To investigate the primary involvement of the PNS in DM1, we previously analyzed DM300 transgenic mice carrying 350 to 500 CTG repeats and displaying a mild DM1 phenotype and found that those mice do not exhibit sensory or motor neuropathy (1). To explore this issue further, we examined new transgenic mice carrying more than 1,300 CTGs and displaying more severe DM1 features (22).

MATERIALS AND METHODS

All animal procedures were conducted according to local guidelines for care and use of experimental animals, and all analyses and measurements were performed blinded to animal genotype.

Generation of DMSXL Transgenic Mice

Production of transgenic mice carrying the human genomic DM1 region with expanded repeats of approximately 350 to 500 CTGs has been reported (23). The mice are of a mixed background. Heterozygous, homozygous, and wild-type mice are obtained from the same litter. Recently, new transgenic mice carrying more than 1,300 CTG repeats were obtained, resulting from large expansions of the CTG repeat in successive generations. The newly generated mice (called *DMSXL*) display a severe phenotype: 1) they are remarkably

From the Department of Clinical Neurosciences (PAP, MK, TK, IBW), University Hospital; Department of Cell Biology and Morphology (RK, IBW), University of Lausanne, Lausanne, Switzerland; and INSERM (GG), U781, Université René Descartes, Hôpital Necker-Enfants Malades, Paris, France.
Send correspondence and reprint requests to: Ibtissam Barakat-Walter, PhD, Department of Clinical Neurosciences, rue du Bugnon 9, 1005 Lausanne, Switzerland; E-mail: Ibtissam.Walter@unil.ch
This work was supported by the Association Française contre les Myopathies.

small; 2) they exhibit muscles abnormalities such as myotonia and muscle weakness; 3) they display abnormalities in the metabolism of multiple messenger RNAs, notably in brain, heart, and muscle; 4) their skeletal muscle showed abnormal splicing patterns for the insulin receptor and chloride channel 1 transcripts; 5) and they have a very high mortality rate, approximately 60% of them die before 7 months of age (22). Because heterozygous mice expressing a low level of *DMPK* transcripts have no obvious phenotype (22), only homozygous transgenic mice were used. Wild-type mice from the same litter were analyzed because they provide the best controls.

Electrophysiologic Studies

Electrophysiologic investigations were carried out with a Viking III EMG machine (Nicolet Biomedical Inc, Madison, WI), using platinum subdermal electrodes (10 mm/30 gauge) for stimulation, recording, and grounding. Sixteen mice (8 DMSXL mice with a body weight of 22.19 ± 2.5 g and 8 wild-type control mice with a body weight of 31.75 ± 3.06 g), aged 5 to 6 months, were studied. Each animal was anesthetized with ketamine (100 mg/kg) and xylazine (10 mg/kg) and fixed in the prone position. Right and left sciatic nerves were stimulated to record the supramaximal motor responses or compound muscle action potentials (CMAPs) from hind limb muscles (flexor digitorum brevis, gastrocnemius, and tibialis anterior), as previously described (24). Compound muscle action potential area and amplitude were measured using the negative peak and onset latency methods. To measure nerve conduction velocity (NCV) of the sciatic nerve, the stimulating electrodes were placed proximally near the sciatic nerve at the level of the limb girdle and distally at the level of the ankle with the recording electrodes placed just over the flexor digitorum brevis.

Animal Perfusion and Tissue Preparation

After electrophysiologic studies, the mice were deeply anesthetized and then transcardially perfused with 0.1-mol/L phosphate-buffered saline (PBS) containing 0.1% heparin and 0.1% procaine, followed by a solution of 4% paraformaldehyde in 0.1-mol/L PBS at pH 7.4. Sciatic nerves, lumbar spinal cord, and hind limb muscles (gastrocnemius and tibialis anterioris) were removed from each animal. To prepare cryostat sections, tissues were first cryoprotected in 30% sucrose overnight, frozen in liquid N_2, and stored at −80°C. For semithin section preparation, the tissues were placed in 2% OsO_4 in PBS for 3 hours, followed by dehydration in a series of graded ethanols and embedded in Epon (1, 25).

Sciatic Nerve Section Analysis

For histologic and morphometric analysis, 1-μm-thick semithin transverse sections were cut from the common trunk of sciatic nerves and stained with toluidine blue. Neurolucida Software and StereoInvestigator program (both from MBF Bioscience, Williston, VT) were used to measure the area of nerve cross sections and the diameter of myelinated axons and to count the total number of myelinated axons on 10 nerve sections from 5 DMSXL and 5 wild-type control mice as described (1, 25).

To count only myelinated motor fibers, cryostat sciatic nerve sections (12 μm) were prepared and double immunolabeled with polyclonal anti–choline acetyltransferase antibody, which stains only myelinated motor fibers (ChAT, 1:50; AB144P, Millipore, Billerica, MA) and anti–neurofilament proteins (NF 200 kd, 1:500; AB1982, Millipore), which stains all myelinated fibers. The sections were incubated with secondary antibody, Alexa Fluor 488 Donkey anti-goat 1:200 (Invitrogen, Carlsbad, CA) and Cy3-conjugated donkey anti-rabbit (1:500; Jackson Immuno Research, West Grove, PA). Myelinated motor fibers were counted on 10 different sections (n = 5 for each mouse line) using an image-processing program (ImageJ 1.40; National Institutes of Health, Bethesda, MD) (1, 25).

Analysis and Quantification of Motor Neurons in the Spinal Cord Lumbar Enlargement

The physical disector method was used to estimate the number of motor neurons in 2-mm segments of lumbar spinal cord (26). Adjacent cryostat transverse sections, 20 μm thick, were prepared from lumbar spinal cord segments taken from 5 wild-type and 5 DMSXL mice. Approximately 50 sampling sections, called disector pairs, were prepared from each animal, and every third disector pair was used to count the number of motor neurons. The sections were immunostained with anti-ChAT and were photographed; the images of each disector pair were carefully aligned using Adobe Photoshop and then imported into the ImageJ 1.40 program. Only ChAT-positive neurons in the top section (tops) of the disector pair were marked and counted. The number of the tops was multiplied by 2 to estimate the number of neurons in the disector pair. Because we used every third disector pair, the number of neurons of each studied disector pair was multiplied by 3. Then the estimated number of neurons of 17 disector pairs was combined to obtain the total number of motor neurons present in the 2-mm segment of lumbar spinal cord. All analyses and counts were performed blinded to the animal type. The results were exported to Microsoft Excel (Microsoft Corp, Redmond, WA) for statistical analysis.

To investigate whether the surviving motor neurons of DMSXL mice express pathologic tau protein, cryostat spinal cord sections from control and DMSXL mice were incubated either with monoclonal antibody PHF-1 (developed by Dr Peter Davies, Albert Einstein College of Medicine, NY; dilution 1:500), which specifically recognizes the phosphorylated serines 396 and 404 at the C-terminus of tau protein, or with AT8 monoclonal antibody (Thermo Fisher Scientific, Waltham, MA; dilution 1:1000), which recognizes the phosphorylated serines 199 and 202. Other sections were incubated with tau-1 monoclonal antibody, which recognizes normal tau protein (produced by Dr Beat Riederer, University of Lausanne, Switzerland; dilution 1:10).

Analysis of Neuromuscular Junctions on Hind Limb Muscle Sections

Serial cryostat longitudinal 20-μm-thick sections were prepared from hind limb muscles. First, the sections were incubated for 45 minutes in 1 μg/mL tetramethyl rhodamine-conjugated α-bungarotoxin (α-BTX; Invitrogen, Life Technologies) and then incubated overnight with the primary polyclonal antibody anti-NF 200 kd (1:500; AB1982, Millipore), followed by incubation with the secondary antibody conjugated

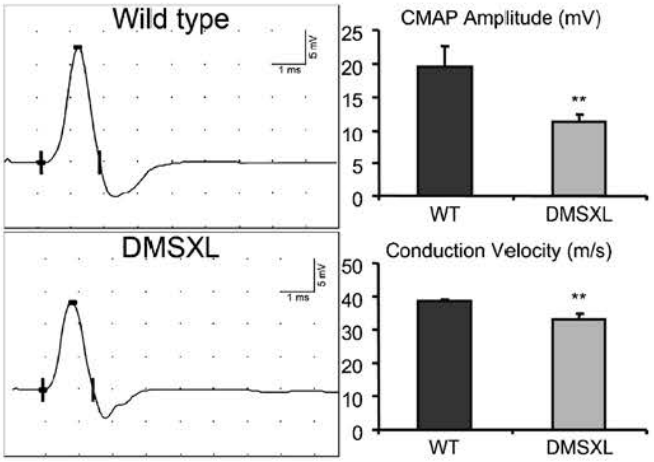

FIGURE 1. Representative recordings of compound muscle action potentials (CMAPs) in gastrocnemius muscle from wild-type and DMSXL mice (left panels). The histogram of mean CMAPs (upper right panel) shows a significant decrease (42%) in CMAP amplitude in DMSXL mice versus wild-type (WT; 11.35 ± 1.11 vs 19.59 ± 2.92, **$p < 0.01$). The mean sciatic nerve conduction velocity is slightly reduced (14%) in DMSXL versus wild-type mice (33.28 ± 1.37 vs 38.75 ± 0.46, **$p < 0.01$) (lower right panel). n = 8 mice/group.

to Alexa Fluor 488 (Invitrogen) for 2 hours (1, 25). Muscle sections were observed by fluorescent microscopy (Axioplan 2; Zeiss; Oberkochen, Germany) and photographed using an image-acquisition program (AxioVision with Axiocam HRc; Zeiss). Images were imported into the ImageJ 1.40 program to analyze all end plates (EPs) in the sections. To avoid counting and measuring the same junction twice, every third section was used. To determine whether the EPs are innervated, we followed the nerve fibers on several sections to determine whether if they made contact with the EP. The percentage of denervated EPs was estimated, and the morphometric parameters (area, shape complexity, and fluorescence intensity of rhodamine–α-BTX labeling) of every EP were measured and calculated as previously described in detail (1, 24, 25). More than 1,400 EPs were measured from each mouse line (n = 6 mice). All analyses and counts were performed blinded to the animal genotype.

Statistical Analysis

Results of DMSXL transgenic mice analysis were compared with the values of wild-type control mice. The distribution of values was checked for normality, and transformations were applied when necessary. Then 1-way analysis of variance was performed followed by the Holm-Bonferroni post hoc test. The distribution of diameters was compared using a χ^2 test. In all performed tests, $p < 0.05$ was considered significant.

RESULTS

Electrophysiologic Evidence of Peripheral Nerve Abnormality in DMSXL Mice

Compound muscle action potentials and NCVs were recorded after sciatic nerve stimulation of both right and left hind limbs from each DMSXL and wild-type mouse. Every DMSXL mouse examined exhibited a decrease in both CMAP parameters and NCV. In DMSXL mice, the amplitude of CMAPs recorded from gastrocnemius muscles was greatly reduced (42%) compared with controls (Fig. 1). There was a similar significant fall in CMAP (38.86%) in tibialis anterior muscles. Moreover, a slowing (14%) of sciatic NCV was observed in DMSXL compared with control mice (Fig. 1). Although the decrease in NCV is slight, it is significant ($p < 0.01$). To rule out the possibility that the reduction in CMAP and NCV in DMSXL mice was due to the small size and weight of these transgenic mice, we measured the CMAP and the NCV in control mice that had a similar size and weight range to the DMSXL. The results demonstrated that the reduction in CMAP and NCV in DMSXL mice was independent of the size and the weight of the mouse. The reduction in CMAP and NCV in DMSXL indicates muscle and nerve dysfunction.

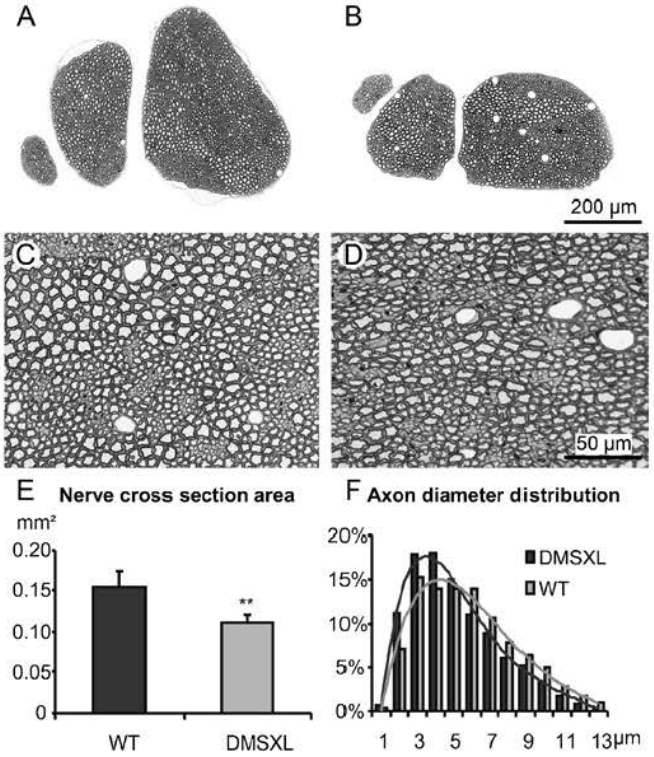

FIGURE 2. Sciatic nerve histology and morphometry. **(A–D)** Transverse semithin sections of sciatic nerve stained with toluidine blue from wild-type (WT) control mice **(A, C)** and DMSXL mice **(B, D)**. The low **(A, B)** and high **(C, D)** magnifications show no obvious structural abnormality in DMSXL sciatic nerves. **(E)** Surface area measurements of nerve sections (from 5 control and 5 DMSXL mice) reveal that mean sciatic nerve section area is significantly smaller in DMSXL mice (0.113 ± 0.011 vs 0.156 ± 0.016 mm², **$p < 0.01$). **(F)** The size-frequency distribution of myelinated axon diameters demonstrates that the peak axon diameter in DMSXL mice is shifted to the left, that is, trend to smaller diameters ($p < 0.001$).

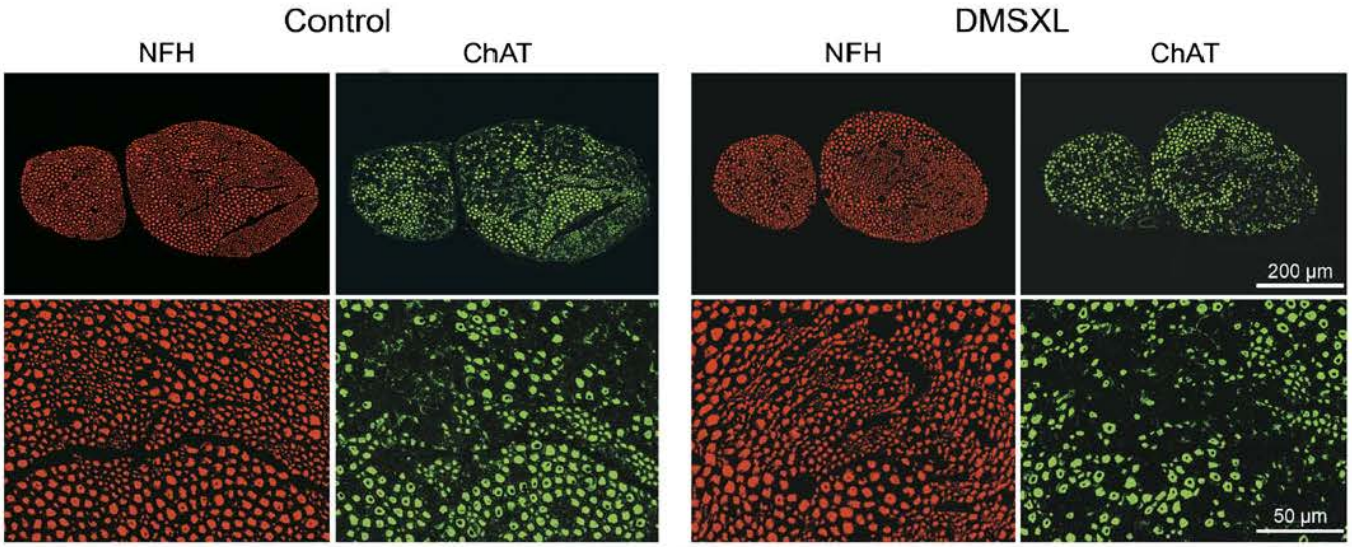

FIGURE 3. Cryostat sciatic nerve cross sections double immunolabeled for neurofilament (NFH) (myelinated axons, red), and anti–choline acetyl transferase (ChAT) (myelinated motor axons, green). In both control and DMSXL mice, low and high magnifications show numerous axons immunolabeled with NFH and not stained with ChAT. Counts of only ChAT-positive axons on 5 nerve sections from 5 wild-type and 5 DMSXL mice revealed a loss of 19% of myelinated motor axons in DMSXL mice.

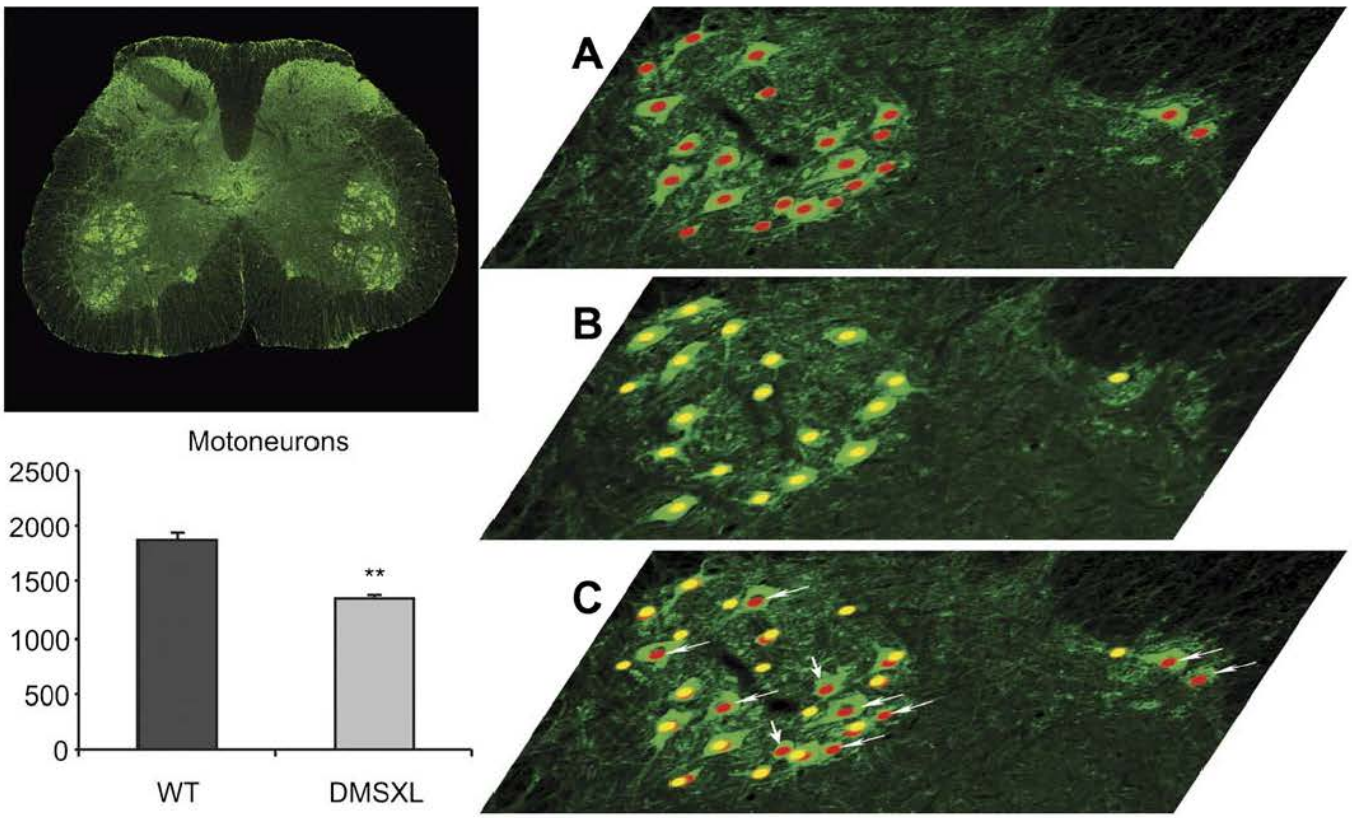

FIGURE 4. Estimation of motor neuron numbers in lumbar spinal cord by the physical disector method. Twenty-micrometer-thick adjacent cryostat transverse sections were prepared from lumbar spinal cord from 5 wild-type (WT) and 5 DMSXL mice. Seventeen disector pairs were analyzed from each animal. Sections were immunolabeled with an anti–choline acetyl transferase (ChAT) antibody. **(A–C)** Micrographs of 1 disector pair: top section **(A)** and bottom section **(B)**. The ChAT-immunolabeled neurons in the top section of the disector pair are marked in red and those in the bottom section are marked in yellow. The marks of the motor neurons in the bottom section are superimposed on the top section **(C)**; arrows indicate the tops (i.e. neurons present only in the top section). The histogram shows that the mean estimated number of motor neurons in DMSXL mice is significantly smaller than in controls (**$p < 0.01$).

Axonopathy and Muscle Dystrophy Underlie the Electrophysiologic Abnormality in DMSXL Mice

Although the general cytoarchitecture of sciatic nerves did not differ noticeably between DMSXL and control mice, the mean area of nerve section in DMSXL mice was smaller than in control mice (0.113 ± 0.011 vs 0.156 ± 0.016 mm^2, $p < 0.01$) (Figs. 2A–E). Moreover, the diameter of myelinated fibers in DMSXL sciatic nerves was smaller, and the thickness of myelin sheath was reduced (19%). The size-frequency histogram based on the measurement of approximately 1,500 fibers from each mouse line showed that the peak axon diameter in DMSXL mice was significantly shifted to a smaller diameter versus that in wild-type mice ($p < 0.001$) (Fig. 2F). In addition, the number of all myelinated fibers in sciatic nerves in DMSXL mice was reduced by 6%. Nevertheless, counts of ChAT-positive axons on sciatic nerve sections double immunolabeled for ChAT and NF revealed a loss of approximately 19% of myelinated motor axons in DMSXL mice (Fig. 3). Because myelinated motor axons represent only 22% of the total number of myelinated axons, the loss of 6% of the total number of myelinated fibers corresponds to a preferential loss of motor axons. Together with the morphometric results, these observations indicate the presence of an axonopathy in DMSXL sciatic nerves with a specific loss of large myelinated fibers. These results were independent of the size and weight of the mice.

Evidence of Motor Neuronopathy in the Lumbar Spinal Cord of DMSXL Mice

To verify whether the loss of motor axons observed in DMSXL mice resulted from only a degeneration of myelinated motor axons (''dying back neuropathy'') or rather from neuronopathy that affects neuron cell bodies, we used the physical disector method to estimate the number of motor neurons in lumbar enlargement of spinal cord (Fig. 4). There was a 24% reduction in the number of motor neurons in DMSXL mice versus controls (1,348 ± 49 vs 1,758 ± 79, $p < 0.01$). These results indicate that the lumbar motor neurons in DMSXL mice are affected by a neuronopathy.

Because tau abnormalities are found in brain neurons of DM patients, we performed immunohistochemical staining for pathologic and normal tau proteins. Incubation of spinal cord sections with PHF-1 or AT8 antibodies demonstrated that, in DMSXL mice, most surviving motor neurons displayed a strong immunostaining (Figs. 5B, D), whereas in control wild-type mice, all motor neurons were PHF-1 and AT8 negative (Figs. 5A, C). In contrast, the normal tau protein was highly expressed in control motor neurons compared with DMSXL motor neurons (Figs. 5E, F). A link between overexpression of a kinase in DM brain neurons and the presence of abnormal tau protein has been reported (27).

Pathologic Changes in the Structure of Neuromuscular Junctions in DMSXL Mice

Histologic examination of gastrocnemius muscle sections labeled with rhodamine–α-BTX and NF antibody showed that control mice displayed EPs with a typical pretzel shape and strong fluorescent labeling, with 98% of them in direct contact with the nerve terminal (Figs. 6A–C). In DMSXL mice, however, numerous EPs exhibited lengthened shapes and faint labeling, and only 77% had axonal terminal contact (Figs. 6D–F). Morphometric analysis showed a significant decrease in the size (16.4%) and shape complexity (17.5%) of EPs in DMSXL mice (Figs. 6G, H). Moreover, the concentration of acetylcholine receptors on postsynaptic membranes assessed by measuring the α-BTX fluorescence labeling intensity was reduced by 23% (Fig. 6I).

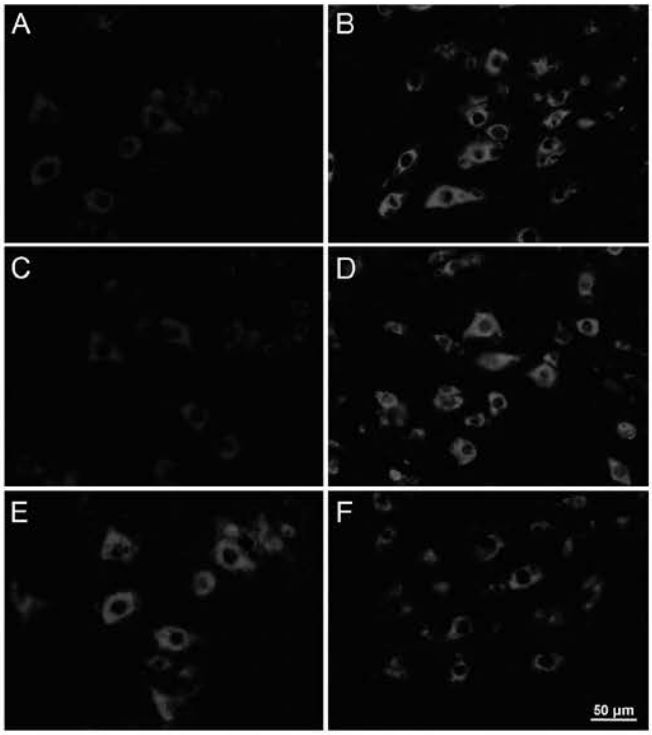

FIGURE 5. Immunocytochemical detection of pathologic hyperphosphorylated and normal tau proteins in spinal cord motor neurons. **(A–E)** Cryostat sections from lumbar spinal cord of wild-type **(A, C, E)** and DMSXL mice **(B, D, F)** immunostained with PHF-1 **(A, B)**, AT8 **(C, D)**, or tau-1 **(E, F)** antibodies. Pathologic hyperphosphorylated tau proteins are highly expressed in motor neurons in DMSXL mice as demonstrated by strong PHF-1 **(B)** or AT8 **(D)** staining. Wild-type mice motor neurons do not show visible PHF-1 **(A)** or AT8 **(C)** staining. Normal tau protein is intensely expressed in wild-type motor neurons **(E)** and is faintly expressed in DMSXL motor neurons **(F)**. Data are representative of 5 mice/group.

DISCUSSION

Involvement of the CNS and other organs in patients with DM1 is well known, but PNS involvement in DM1 remains controversial. Clinically, the diagnosis of peripheral neuropathy in patients with DM1 is mainly detected by electrophysiologic tests and supported by neurologic examination. Several reports have described a reduction in CMAP, a slowing of maximal and minimal motor NCV, or an increase in the minimal latency of F waves in DM patients, suggesting the presence of pathologic changes in peripheral nerves

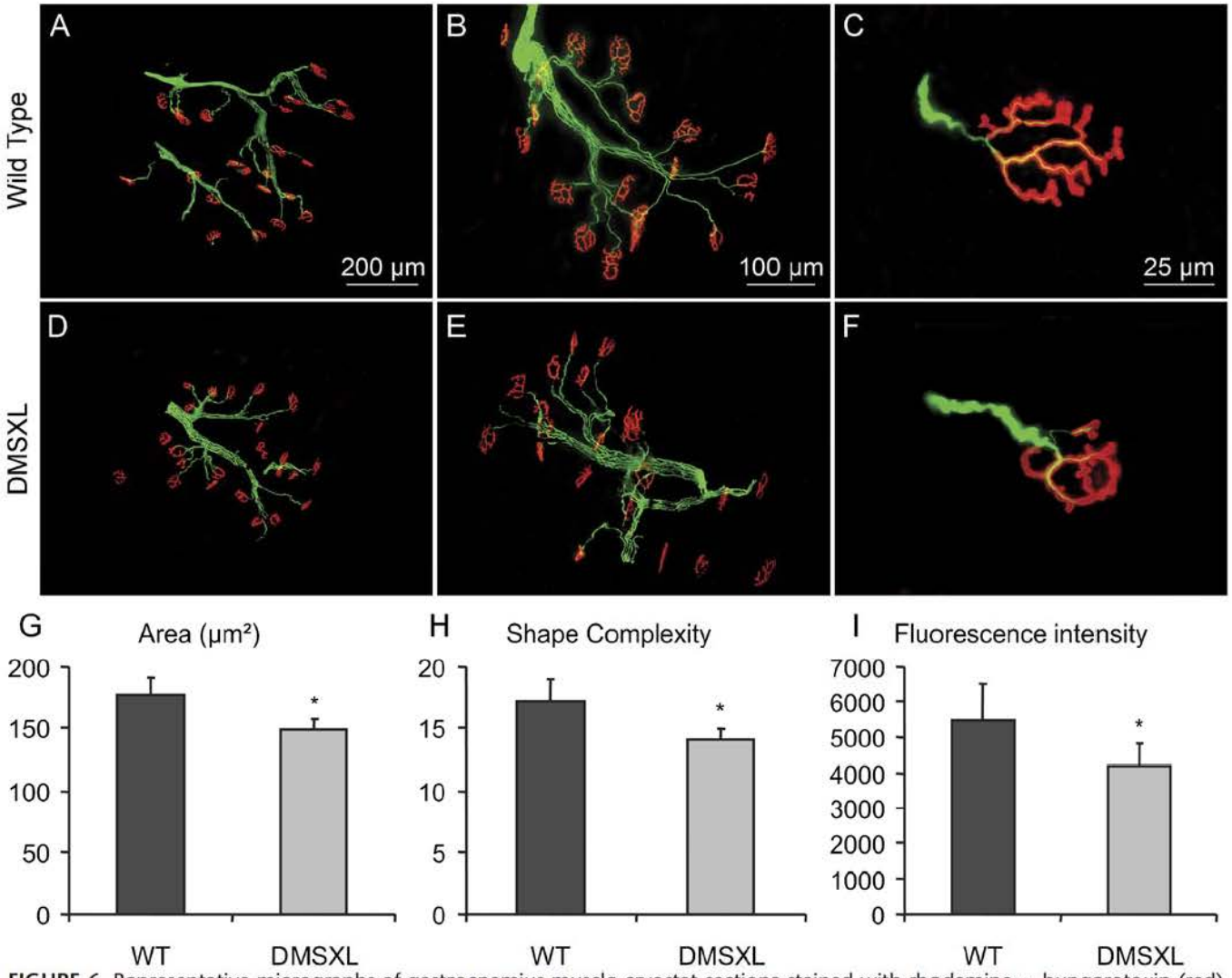

FIGURE 6. Representative micrographs of gastrocnemius muscle cryostat sections stained with rhodamine–α-bungarotoxin (red) and neurofilament antibody (green). **(A–F)** In wild-type mice (WT), nearly all end plates (EPs) are innervated by branches of axons **(A, B)**. End plates without any contact to axon terminals are easily identified in DMSXL mice **(D, E)**. At higher magnification, representative images illustrate a single EP **(C, F)**. In a DMSXL mouse **(F)**, the EP has a smaller size and a less complex shape than that in a control mouse **(C)**. **(G–I)** The mean surface area of EPs, the shape complexity, and the density of acetylcholine receptors on postsynaptic membranes labeled with rhodamine–α-BTX (fluorescence intensity) are represented in the 3 histograms. More than 1,400 EPs were measured from each mouse line. All 3 parameters were smaller in DMSXL mice versus WT control mice (*$p < 0.05$).

(12–16, 28–33). Indeed, a few histopathologic studies of peripheral nerves and muscle biopsies have confirmed the presence of peripheral neuropathy in patients with DM1 (34–40). Some authors who support the presence of neuropathy in DM1 argue that pathologic changes and peripheral nerve dysfunction are primary and are unrelated to the glucose intolerance (which may be present in some patients with DM1) or to other metabolic, nutritional, or genetic factors (12, 31, 41). The absence of impairment of nerve conduction in patients with DM1 has also been reported (17, 19, 21). These and other authors found no evidence of morphologic abnormality of peripheral nerves, no signs of muscles denervation, and no loss in the number of motor neurons in patients with DM1 (18, 20, 21). It is important to emphasize that studies confirming or denying association of peripheral neuropathy with DM1 disease involved patients of unknown genotype because the molecular basis of DM1 was not yet identified when those reports appeared. Consequently, the earlier studies did not take into consideration the relationship between the expansion of the CTG repeat and the severity of the clinical features. Therefore, we believe that the conflicting results are probably due to different lengths of CTG repeats in the patients.

We previously studied transgenic mice (DM300) carrying 350 to 500 CTG repeats and displaying mild DM1 features (23, 42), and analysis of the sciatic nerve, lumbar dorsal root

ganglia, and spinal cord of those mice revealed neither axonopathy nor neuronopathy (1). Moreover, no significant changes can be detected either in CMAP index or in NCV in DM300 transgenic mice (43). These results suggest that the length of CTG repeats (350–500) probably was not sufficient to induce peripheral neuropathy in that mouse model (1).

Because CMAP amplitude represents the total number of stimulated axons and NCV provides information about the rate at which a neural impulse propagates along myelinated fibers (44), the reduction in CMAP amplitude and NCV detected in DMSXL mice indicates nerve dysfunction. This correlates with clinical studies that found peripheral nerve dysfunction in patients with DM1 (12–16, 29, 32, 33). Structural pathologic changes that probably caused the dysfunction of peripheral nerves in the mice were detected in sciatic nerves, lumbar motor neurons, and neuromuscular junctions. In particular, the size-frequency distribution of myelinated fiber diameters indicates that the 6% reduction in the total number of myelinated fibers in DMSXL mice was essentially a loss of large axons, which correspond to motor fibers in sciatic nerve (45). The reduction of 19% of ChAT-positive axons confirmed a preferential loss of motor axons, and the decrease in the number of motor neuron cell bodies indicates the presence of a motor neuronopathy. Moreover, the higher expression of hyperphoshorylated tau protein in DMSXL mice motor neurons argues for increased kinase activity (27). It is worth noting that comparable motor neuronopathy and pathologic changes in neuromuscular junctions have been described in patients with DM1 (46). Indeed, Wheeler et al. (46) demonstrated the presence of ribonuclear foci in motor neurons spinal cord autopsy and the high expression of CUGexp RNA and sequestration of MBNL1 protein in postsynaptic nuclei of neuromuscular junctions in muscle biopsies. Other studies have emphasized that dramatic changes in tau isoform expression in brain neurons is associated with the presence of large CTG expansion in the brains of patients with DM1 (27, 47–49); the expanded CUG repeats may affect RNA metabolism of several genes and act as a gain-of-function mutation (48).

We believe that the motor neuropathy detected in DMSXL mice is independent of possible alterations in the thyroid or pancreatic β-cell function because the DM300 transgenic mice used to generate DMSXL mice did not develop either motor or sensory neuropathy (1). Moreover, the neuropathy detected in DMSXL transgenic mice showed a loss in the number of motor neurons, whereas neuropathies induced by hypothyroidism or diabetes are mainly characterized by a deficiency in myelination and progressive distal loss of axonal terminals but without perikaryal loss (50, 51). Our data are consistent with other studies demonstrating a selective loss of functioning motor units and alterations of neuromuscular excitability in patients with DM1 (52–55).

Genotype-phenotype correlation studies also report that muscular disability and the severity of hand muscle myotonia depend on the CTG repeat length in leukocyte DNA (56–61). The severity of cardiac conduction abnormalities and arrhythmia in DM1 is also directly related to age and CTG repeat length (62). Moreover, an association between the CTG repeat size and cognitive impairment has been described (63, 64). Because transgenic mice carrying 350 to 500 CTG repeat did not have peripheral neuropathy (1), whereas DMSXL mice undoubtedly have motor neuropathy, we conclude that there is a correlation between the development of neuropathy in DM1 transgenic mice and the size of the CTG triplet. However, it should be noted that the relationship between the length of the CTG repeat and the severity of DM1 features does not always hold true, and there are some exceptions. Indeed, some authors claim that cataract, gastrointestinal, respiratory insufficiency sleep disorder, and other DM features are not correlated with the length of the CTG triplet (56, 58). Because in DM1-affected individuals the instability of the triplet repeats induces somatic heterogeneity characterized by a variable size in different tissues, some investigators hypothesize that the somatic mosaicism might be one possible explanation for the lack of precise correlation between the number of CTG repeats in leukocyte DNA and the severity of DM1 in its multisystemic aspect.

In conclusion, analyses of DMSXL transgenic mice carrying a large CTG expansion and expressing a severe DM1 phenotype provide evidence that these mice have a motor neuropathy that we infer to be linked to their large CTG expansion. In the future, we will investigate whether sensory neuropathy can also be linked to the long CTG repeat and severe form of DM1.

ACKNOWLEDGMENTS

The authors thank Dr M. Price for critical reading of the article and Drs P. Davies and B. Riederer for providing the PHF-1 and tau-1 antibodies.

REFERENCES

1. Gantelet E, Kraftsik R, Delaloye S, et al. The expansion of 300 CTG repeats in myotonic dystrophy transgenic mice does not induce sensory or motor neuropathy. *Acta Neuropathol* 2007;114:175–85
2. Harper PS. *Myotonic Dystrophy*. Philadelphia: Saunders WB, 2001
3. Fu YH, Pizzuti A, Fenwick RG Jr, et al. An unstable triplet repeat in a gene related to myotonic muscular dystrophy. *Science* 1992;255:1256–58
4. Mahadevan M, Tsilfidis C, Sabourin L, et al. Myotonic dystrophy mutation: An unstable CTG repeat in the 3′ untranslated region of the gene. *Science* 1992;255:1253–55
5. Hunter A, Tsilfidis C, Mettler G, et al. The correlation of age of onset with CTG trinucleotide repeat amplification in myotonic dystrophy. *J Med Genet* 1992;29:774–79
6. Sahgal V, Bernes S, Sahgal S, et al. Skeletal muscle in preterm infants with congenital myotonic dystrophy. Morphologic and histochemical study. *J Neurol Sci* 1983;59:47–55
7. Abe T, Sato M, Kuboki J, et al. Lens epithelial changes and mutated gene expression in patients with myotonic dystrophy. *Br J Ophthalmol* 1999; 83:452–57
8. Hiromasa S, Ikeda T, Kubota K, et al. Ventricular tachycardia and sudden death in myotonic dystrophy. *Am Heart J* 1988;115:914–15
9. van Spaendonck KP, Ter Bruggen JP, Weyn Banningh EW, et al. Cognitive function in early adult and adult onset myotonic dystrophy. *Acta Neurol Scand* 1995;91:456–61
10. Zifko UA, Hahn AF, Remtulla H, et al. Central and peripheral respiratory electrophysiological studies in myotonic dystrophy. *Brain* 1996;119: 1911–22
11. Meola G, Sansone V. Cerebral involvement in myotonic dystrophies. *Muscle Nerve* 2007;36:294–306
12. Bae JS, Kim OK, Kim SJ, et al. Abnormalities of nerve conduction studies in myotonic dystrophy type 1: Primary involvement of nerves or incidental coexistence? *J Clin Neurosci* 2008;15:1120–24

13. Jamal GA, Weir AI, Hansen S, et al. Myotonic dystrophy. A reassessment by conventional and more recently introduced neurophysiological techniques. *Brain* 1986;109:1279–96
14. Krishnan AV, Kiernan MC. Axonal function and activity-dependent excitability changes in myotonic dystrophy. *Muscle Nerve* 2006;33: 627–36
15. Mondelli M, Rossi A, Malandrini A, et al. Axonal motor and sensory neuropathy in myotonic dystrophy. *Acta Neurol Scand* 1993;88:141–48
16. Roohi F, List T, Lovelace RE. Slow motor nerve conduction in myotonic dystrophy. *Electromyogr Clin Neurophysiol* 1981;21:97–105
17. Caruso G, Ferrannini E. Conventional electromyography in myotonic dystrophy. *Riv Patol Nerv Ment* 1976;97:263–76
18. Drachman DB, Fambrough DM. Are muscle fibers denervated in myotonic dystrophy? *Arch Neurol* 1976;33:485–88
19. Messina C, Tonali P, Scoppetta C. [Electrophysiological observations in dystrophia myotonica and distal myopathy]. *Riv Neurol* 1976;46: 542–52
20. Pollock M, Dyck PJ. Peripheral nerve morphometry in myotonic dystrophy. *Arch Neurol* 1976;33:33–39
21. Walton JN, Irving D, Tomlinson BE. Spinal cord limb motor neurons in dystrophia myotonica. *J Neurol Sci* 1977;34:199–211
22. Gomes-Pereira M, Foiry L, Nicole A, et al. CTG trinucleotide repeat "big jumps": Large expansions, small mice. *PLoS Genet* 2007;3:e52
23. Seznec H, Agbulut O, Sergeant N, et al. Mice transgenic for the human myotonic dystrophy region with expanded CTG repeats display muscular and brain abnormalities. *Hum Mol Genet* 2001;10:2717–26
24. Panaite PA, Barakat-Walter I. Thyroid hormone enhances transected axonal regeneration and muscle reinnervation following rat sciatic nerve injury. *J Neurosci Res* 2010;88:1751–63
25. Panaite PA, Gantelet E, Kraftsik R, et al. Myotonic dystrophy transgenic mice exhibit pathologic abnormalities in diaphragm neuromuscular junctions and phrenic nerves. *J Neuropathol Exp Neurol* 2008;67:763–72
26. Sterio DC. The unbiased estimation of number and sizes of arbitrary particles using the disector. *J Microsc* 1984;134:127–36
27. Vermersch P, Sergeant N, Ruchoux MM, et al. Specific tau variants in the brains of patients with myotonic dystrophy. *Neurology* 1996;47:711–17
28. Hermans MC, Faber CG, Vanhoutte EK, et al. Peripheral neuropathy in myotonic dystrophy type 1. *J Peripher Nerv Syst* 2011;16:24–29
29. Mechler F, Csenker E, Fekete I, et al. Electrophysiological studies in myotonic distrophy. *Electromyogr Clin Neurophysiol* 1982;22:349–56
30. Mongia SK, Lundervold A. Electrophysiological abnormalities in cases of dystrophia myotonica. *Eur Neurol* 1975;13:360–76
31. Olson ND, Jou MF, Quast JE, et al. Peripheral neuropathy in myotonic dystrophy. Relation to glucose intolerance. *Arch Neurol* 1978;35:741–45
32. Panayiotopoulos CP, Scarpalezos S. Dystrophia myotonica. A model of combined neural and myopathic muscle atrophy. *J Neurol Sci* 1977;31: 261–68
33. Rossi B, Sartucci F, Stefanini A, et al. Measurement of motor conduction velocity with Hopf's technique in myotonic dystrophy. *J Neurol Neurosurg Psychiatry* 1983;46:93–95
34. Allen DE, Johnson AG, Woolf AL. The intramuscular nerve endings in dystrophia myotonica—A biopsy study by vital staining and electron microscopy. *J Anat* 1969;105:1–26
35. Cros D, Harnden P, Pouget J, et al. Peripheral neuropathy in myotonic dystrophy: A nerve biopsy study. *Ann Neurol* 1988;23:470–76
36. Engel AG, Jerusalem F, Tsujihata M, Gomez MR. The neuromuscular junction in myopathies. A quantitative ultrastructural study. In: Brisson E, ed. *Recent Advances in Mycology*, Amsterdam, Netherlands: Excerpta Medica, 1975:132–43
37. McComas AJ, Sica RE, Campbell MJ. "Sick" motoneurones. A unifying concept of muscle disease. *Lancet* 1971;1:321–26
38. von Giesen HJ, Stoll G, Koch MC, et al. Mixed axonal-demyelinating polyneuropathy as predominant manifestation of myotonic dystrophy. *Muscle Nerve* 1994;17:701–3
39. Wang JF, Schroder JM. Comparative morphometric evaluation of peripheral nerves and muscle fibers in myotonic dystrophy. *Acta Neuropathol* 2000;99:39–47
40. MacDermoth V. The histology of the neuromuscular junction in dystrophia myotonica. *Brain* 1961;84:75–84
41. Pfeilsticker BH, Bertuzzo CS, Nucci A. Electrophysiological evaluation in myotonic dystrophy: Correlation with CTG length expansion. *Arq Neuropsiquiatr* 2001;59:186–91
42. Vignaud A, Ferry A, Huguet A, et al. Progressive skeletal muscle weakness in transgenic mice expressing CTG expansions is associated with the activation of the ubiquitin-proteasome pathway. *Neuromuscul Disord* 2010;20:319–25
43. Gantelet E. Are myotonic dystrophy and peripheral neuropathy associated? Morphological, morphometric and electrophysiological analysis in DM1 transgenic mice. PhD thesis, University of Lausanne, Switzerland, 2007.
44. Dumitru D, Amato AA, Zwarts M. Nerve conduction studies. In: Dumitru D, Amato AA, Zwarts M, eds. *Electrodiagnostic Medicine*. Philadelphia, PA: Hanley & Belfus Inc, 2002:159–224
45. Schmalbruch H. Fiber composition of the rat sciatic nerve. *Anat Rec* 1986;215:71–81
46. Wheeler TM, Krym MC, Thornton CA. Ribonuclear foci at the neuromuscular junction in myotonic dystrophy type 1. *Neuromuscul Disord* 2007;17:242–47
47. Maurage CA, Udd B, Ruchoux MM, et al. Similar brain tau pathology in DM2/PROMM and DM1/Steinert disease. *Neurology* 2005;65:1636–38
48. Sergeant N, Sablonniere B, Schraen-Maschke S, et al. Dysregulation of human brain microtubule-associated tau mRNA maturation in myotonic dystrophy type 1. *Hum Mol Genet* 2001;10:2143–55
49. Ashizawa T, Dubel JR, Dunne PW, et al. Anticipation in myotonic dystrophy. II. Complex relationships between clinical findings and structure of the GCT repeat. *Neurology* 1992;42:1877–83
50. Legrand J. Thyroid hormone effects on growth and development. In: Henneman G, ed. *Thyroid Hormone Metabolism*. New York, NY: Marcel Dekker; 1986:503–34
51. Ramji N, Toth C, Kennedy J, et al. Does diabetes mellitus target motor neurons? *Neurobiol Dis* 2007;26:301–11
52. Boerio D, Hogrel JY, Bassez G, et al. Neuromuscular excitability properties in myotonic dystrophy type 1. *Clin Neurophysiol* 2007;118:2375–82
53. McComas AJ, Sica RE, Toyonaga K. Incidence, severity, and time-course of motoneurone dysfunction in myotonic dystrophy: Their significance for an understanding of anticipation. *J Neurol Neurosurg Psychiatry* 1978;41:882–93
54. Hansen S, Ballantyne JP. A quantitative electrophysiological study of motor neurone disease. *J Neurol Neurosurg Psychiatry* 1978;41:773–83
55. Ballantyne JP, Hansen S. New method for the estimation of the number of motor units in a muscle. 2. Duchenne, limb-girdle and facioscapulohumeral, and myotonic muscular dystrophies. *J Neurol Neurosurg Psychiatry* 1974;37:1195–201
56. Jaspert A, Fahsold R, Grehl H, et al. Myotonic dystrophy: Correlation of clinical symptoms with the size of the CTG trinucleotide repeat. *J Neurol* 1995;242:99–104
57. Logigian EL, Moxley RT, Blood CL, et al. Leukocyte CTG repeat length correlates with severity of myotonia in myotonic dystrophy type 1. *Neurology* 2004;62:1081–89
58. Marchini C, Lonigro R, Verriello L, et al. Correlations between individual clinical manifestations and CTG repeat amplification in myotonic dystrophy. *Clin Genet* 2000;57:74–82
59. Redman JB, Fenwick RG Jr, Fu YH, et al. Relationship between parental trinucleotide GCT repeat length and severity of myotonic dystrophy in offspring. *JAMA* 1993;269:1960–65
60. Timchenko NA, Patel R, Iakova P, et al. Overexpression of CUG triplet repeat-binding protein, CUGBP1, in mice inhibits myogenesis. *J Biol Chem* 2004;279:13129–39
61. Tsilfidis C, MacKenzie AE, Mettler G, et al. Correlation between CTG trinucleotide repeat length and frequency of severe congenital myotonic dystrophy. *Nat Genet* 1992;1:192–95
62. Finsterer J, Gharehbaghi-Schnell E, Stollberger C, et al. Relation of cardiac abnormalities and CTG-repeat size in myotonic dystrophy. *Clin Genet* 2001;59:350–55
63. Sistiaga A, Urreta I, Jodar M, et al. Cognitive/personality pattern and triplet expansion size in adult myotonic dystrophy type 1 (DM1): CTG repeats, cognition and personality in DM1. *Psychol Med* 2010;40:487–95
64. Winblad S, Lindberg C, Hansen S. Cognitive deficits and CTG repeat expansion size in classical myotonic dystrophy type 1 (DM1). *Behav Brain Funct* 2006;2:16